J. Ocean Univ. China (Oceanic and Coastal Sea Research)
DOI 10.1007/s11802-017-3061-x
ISSN 1672-5182, 2017 16 (3): 447-454
http://www.ouc.edu.cn/xbywb/
E-mail:xbywb@ouc.edu.cn

Quantification of Methane Fluxes from Hydrocarbon Seeps to the Ocean and Atmosphere: Development of an *in situ* and Online Gas Flux Measuring System

DI Pengfei[1), *], CHEN Qinghua[1)], and CHEN Duofu[1), 2), *]

1) *CAS Key Laboratory of Marginal Sea Geology*, *South China Sea Institute of Oceanology*, *Chinese Academy of Sciences*, *Guangzhou* 510301, *P. R. China*
2) *Shanghai Engineering Research Center of Hadal Science and Technology*, *College of Marine Sciences*, *Shanghai Ocean University*, *Shanghai* 201306, *P. R. China*

(Received November 18, 2015; revised January 1, 2017; accepted January 11, 2017)

Abstract Natural hydrocarbon seeps in the marine environment are important contributors to greenhouse gases in the atmosphere. Such gases include methane, which plays a significant role in global carbon cycling and climate change. To accurately quantify the methane flux from hydrocarbon seeps on the seafloor, a specialized in situ and online gas flux measuring (GFM) device was designed to obtain high-resolution time course gas fluxes using the process of equal volume exchange. The device consists of a 1.0-m diameter, 0.9-m tall, inverted conical tent and a GFM instrument that contains a solenoid valve, level transducer, and gas collection chamber. Rising gas bubbles from seeps were measured by laboratory-calibrated GFM instruments attached to the top of the tent. According to the experimental data, the optimal anti-shake time interval was 5 s. The measurement range of the device was 0–15 L min^{-1}, and the relative error was ± 1.0%. The device was initially deployed at an active seep site in the Lingtou Promontory seep field in South China Sea. The amount of gas released from a single gas vent was 30.5 m^3 during the measurement period, and the gas flow rate ranged from 22 to 72 L h^{-1}, depending on tidal period, and was strongly negatively correlated with water depth. The measurement results strongly suggest that oceanic tides and swells had a significant forcing effect on gas flux. Low flow rates were associated with high tides and vice versa. The changes in gas volume escaping from the seafloor seeps could be attributed to the hydrostatic pressure induced by water depth. Our findings suggest that in the marine environment, especially in the shallow shelf area, sea level variation may play an important role in controlling methane release into the ocean. Such releases probably also affect atmospheric methane levels.

Key words hydrocarbon seeps; GFM device; *in situ*; equal volume exchange; Methane flux; South China Sea

1 Introduction

Natural marine hydrocarbon seeps are widely distributed on the seabed of almost all continental margins (Campbell, 2006; Judd *et al*., 2002, 2003; Judd and Hovland, 2007; Boetius and Wenzhöfer, 2013; Suess, 2014). Seeps are the main pathways or conduits for the transfer of fossil geologic carbon, primarily methane (CH_4), from the lithosphere to the hydrosphere and atmosphere. Methane has a 23-fold higher potential to induce global warming than an equal quantity of carbon dioxide over a 100-year timescale, and it may have an important impact on global climate change (Ramaswamy *et al*., 2001; Dimitrov, 2003; Etiope and Milkov, 2004; Etiope *et al*., 2008). Approximately 582 ± 87 Tg of CH_4 is added to the atmosphere annually (Etiope *et al*., 2008). As a result of the ocean's effective CH_4 biofilter, which includes both anaerobic and aerobic microbial CH_4 consumption in sediments and seawater, only 4–20 Tg yr^{-1} of methane is discharged into the atmosphere from the ocean (Judd, 2004; Kvenvolden and Rogers, 2005; Solomon *et al*., 2007; Etiope, 2009). This amount is approximately half of the global geological methane emissions of 40–60 Tg yr^{-1} (Etiope *et al*., 2008; Etiope, 2009). However, there are significant uncertainties in these values because few hydrocarbon seep fields have been studied. Therefore, accurate quantification of the methane fluxes from seafloor seeps is necessary to evaluate their influence on the global methane budget and global climate change. However, progress in quantifying the total methane flux released into the ocean and atmosphere via this pathway has been hindered because of limited technology and methods.

Recently, much attention has been paid to long-term in situ and online methods that can be adapted to measure methane fluxes from seafloor seeps. Several different

* Corresponding authors. Tel: 0086-20-85290286; 89105350
E-mail: pfd@scsio.ac.cn; cdf@gig.ac.cn

devices have been developed to make such measurements at various hydrocarbon seep locations. Some examples are the seafloor observatory, which successfully measured the natural gas flux using the quantitative volume method at the Bush Hill seepage area (Robert, 1999, 2001); the gas-capture buoy, which is a floating collector that measures the amount of natural gas bubbles rising to the sea surface (Washburn *et al.*, 2001); the turbine seep tent, which was developed by Ira Leifer to measure the bubble flux at the Bush Hill and Hydrate Ridge seepage areas (Leifer *et al.*, 2003, 2005); the underwater stereoscopic camera system that quantifies bubble characteristics and bubble fluxes at natural seep vents (Leifer *et al.*, 2015; Wang *et al.*, 2015, 2016); and acoustic measuring devices that estimate the gas bubble flux and observe the three-dimensional dynamic distribution of natural gas in seepage areas (Greinert *et al.*, 2004; Nikolovska *et al.*, 2006; Deimling *et al.*, 2010). Moreover, in China, theoretical studies on gas bubble flow in seepage areas have been carried out using acoustic transmission and numerical simulation (Li *et al.*, 2010; Long *et al.*, 2012). However, there remains a lack of long-term in situ and online measuring devices in China.

Recently, many active hydrocarbon seep sites have been found offshore in the northern South China Sea, *e.g.*, the Yinggehai Basin, Pearl River Mouth Basin, Qiongdongnan Basin, Taixinan Basin of the Shenhu area, and Xisha Trough (Chen *et al.*, 2006; Huang *et al.*, 2006; Han *et al.*, 2008; Huang *et al.*, 2009; Di *et al.*, 2012; Chen *et al.*, 2013; Li *et al.*, 2013; Feng and Chen, 2015; Hu *et al.*, 2015; Liang *et al.*, Under Revision). However, few quantitative studies on methane flux, activity characteristics, and influencing factors of hydrocarbon seeps have been previously conducted. Therefore, the main purpose of our study was to develop a novel in situ and online gas flux measuring (GFM) device that can quantify methane fluxes from a hydrocarbon seep. We 1) developed a novel in situ and online GFM device and 2) deployed the device at a shallow active hydrocarbon seep vent in the Yinggehai Basin of the South China Sea (Fig.1).

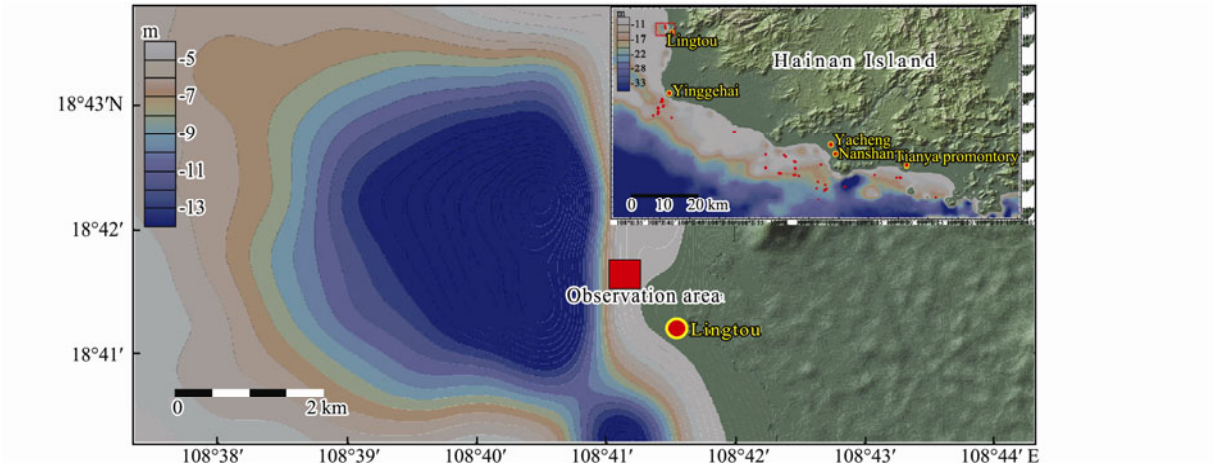

Fig.1 Bathymetric map showing the location of the hydrocarbon seep area where our in situ and online observation was conducted. The yellow dots denote the villages of Lingtou, Yinggehai, Yacheng, Nanshan, and Tianya Promontory (from left to right) in Hainan Province. The red dots denote the distribution of the nearshore hydrocarbon seeps (Huang *et al.*, 2009).

2 GFM Device Design

2.1 Theory of GFM Device

The GFM device was specifically designed for measuring gas fluxes from hydrocarbon seeps in the Yinggehai Basin *via* the process of equal volume exchange (Fig.2). It mainly consists of the GFM system, a storage control system, and data processing software. The measurement process of the GFM device is as follows. Rising bubbles enter the gas collection chamber, expelling an equal volume of seawater in the chamber downward. When the water level decreases to the level of the lower probe (probe 2) in the chamber, a valve opens automatically and the gas in the chamber is instantly released. Then, when the seawater level rises to the level of the higher probe (probe 1), the valve closes automatically and the GFM device resumes collection of gas. The total flux is calculated on the basis of the frequency of the valve opening and the chamber volume, whereas the instantaneous flow rate is calculated on the basis of the time required for a single round of gas collection (Di *et al.*, 2014a, 2014b).

2.2 Description

The GFM device (Fig.2) contained a GFM instrument that is used to quantify gas flux through the tent (Di *et al.*, 2014a, 2014b). The GFM instrument, which was machined out of stainless steel, contained a solenoid valve, level transducer, and gas collection chamber. The level transducer was set vertically inside the chamber, and the solenoid valve was connected to the outside of the chamber. The inside diameter of the chamber section was 9.91 cm. For the deployed seep tents, the total gas flux is calculated based on the frequency of valve opening and the chamber volume, while the instantaneous gas flux is calculated based on the time required for a single round of gas collection.

The GFM instrument was connected to a 1.0 m diame-

ter, 0.9 m tall, inverted conical seep tent made of 1 mm thick stainless steel; this tent was used to collect gas bubbles emitted from a hydrocarbon seep. The bottom support frame was a 0.2 m diameter ring that was welded to the tent's bottom edge. A deployment bridle was attached to four eyebolts on the seep tent as well as two 20 kg diving weights and two sealing capsules attached to the ring at equal spacing. The seep tent was directly deployed onto the seep vents. A metal screen grid was placed inside the tent and below the chamber to block debris and fauna from entering the gas collection chamber and blocking the solenoid valve. A 0.5 cm grid size was chosen after testing to give the best bubble breakup without noticeable gas retention. Under the gas bubble breakup grid were two rods that were used to fix the methane sensor and conductivity-temperature-depth (CTD) sensor.

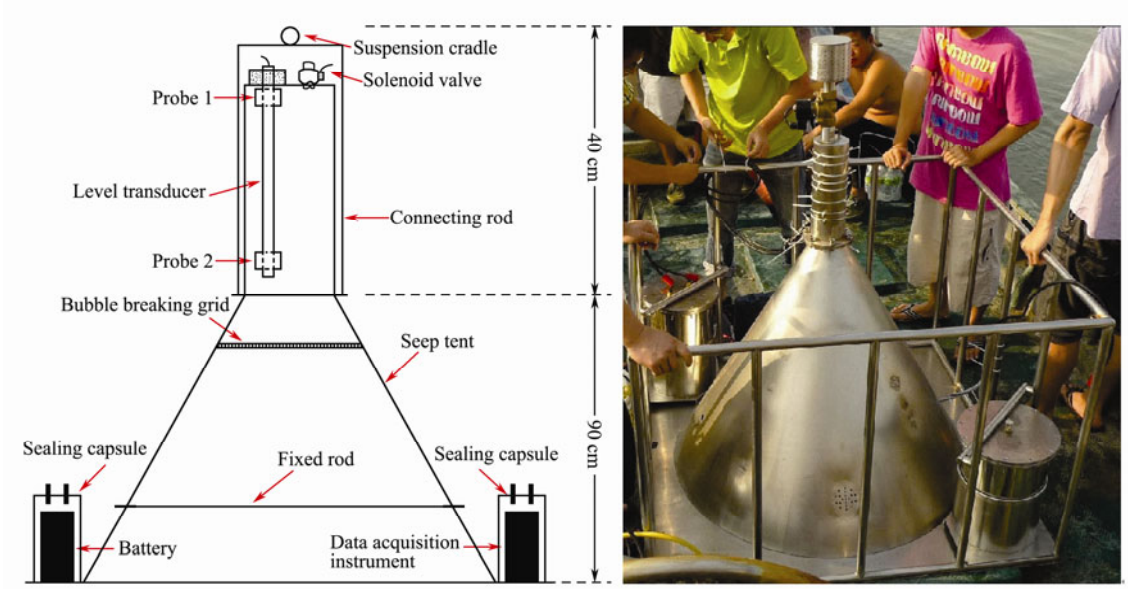

Fig.2 Schematic diagram and photograph of the *in situ* and online gas flux measuring device (Di *et al.*, 2014a, 2014b).

The level transducer and solenoid valve were connected to the storage control system, which was placed in the sealing capsule with two underwater three-conductor (power, ground, and signal) cables with attached rope strain reliefs (Fig.3). The level transducer and solenoid valve require 12 V DC power, and their output signal is recorded by the storage control system. The vertical movement of the level transducer probe sends signals to the control module. The control module then transports the signal to the driver module and the storage module. The driver module controls the opening and closing of the solenoid valve. The storage module records and stores the signal to give a single measurement of gas flux.

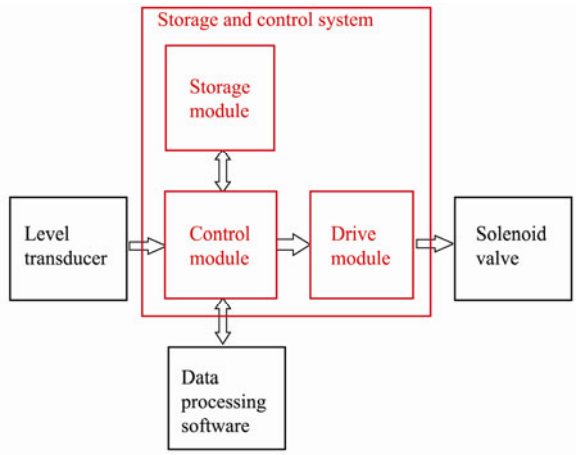

Fig.3 Schematic diagram of the storage control system of the *in situ* and online gas flux measuring device.

2.3 Data Processing Software

Data processing software was used to set the run parameters (current time, running start time, and end time) of the GFM device. It was also used to extract the recorded flux data and save them as a .txt file. The software not only reads the gas flux data but also analyzes and processes the gas flux data. It also can determine the flow rate at any time and display an instantaneous flow rate change curve and integrated flux in real time.

3 Calibration and Error Analysis

3.1 Volume Calibration

The volume of the gas collection chamber is a key parameter for accurately quantifying the methane flux from hydrocarbon seeps. Two methods were adopted to calibrate the volume of the gas collection chamber. Each method was repeated many times and the average of all the measured gas collection chamber volumes was used. One method measured the volume of water drained by the gas in the collection chamber when probe 2 of the level transducer dropped down. The measured volume of the gas collection chamber was 1727.3 mL. Another method measured the volume of water in the inverted gas collection chamber when probe 2 of the level transducer dropped down (Fig.4). With this method, the measured volume of the gas collection chamber was 1822.5 mL. Owing to the vertical movement of probe 2, the water

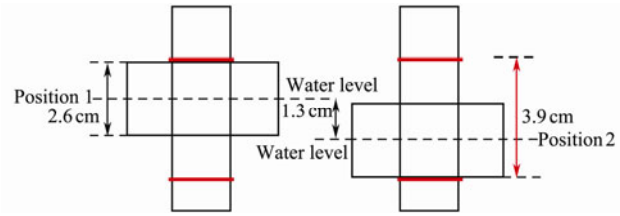

Fig.4 Position of probe 2 and water level in the normal (left) and inverted (right) chambers when the solenoid valve is open.

level at this location changes when the gas collection chamber is placed and inverted (Fig.4). Therefore, the water volume measured by the inverted method is larger than the actual volume of the gas collection chamber (Fig.4). The calibration volume V_C equals the measured volume V_M subtracted from the volume for the half-floating ball height V_H:

$$V_C = V_M - V_H . \quad (1)$$

According to Eq. (1), the calibration volume was 1722.28 mL by the inverted method. Thus, the average calibration volume of the gas collection chamber from the two methods was 1724.79 mL, and the relative error was ± 0.1%.

3.2 Range of Gas Flow Rates and Relative Error Analysis

The range of gas flow rate and relative error were calibrated in a large tank (Fig.5). The large pool (2 m×2 m×2 m) located at the submarine simulative laboratory of GIG, CAS (Guangzhou Institute of Geochemistry, China Academy of Science) was used. An air compressor and a gas mass flow meter spanning 0–200 SCCM (Standard Cubic Centimeters per Minute) (mode: D07-11C, Seven Star Electronics) were connected via an air pipe. The air pipe ran from the controller to the bottom of the tank where it was connected to a 1.5 cm diameter hose placed under the GFM device. The seep tent was placed on top of the bubble source and connected to the data storage and control system. The gas flow rate was measured by an integrating instrument (model: D08-8C/ZM, Seven Star Electronics). This experiment was carried out in an indoor pool at room temperature (25℃). The gas source was compressed air at a pressure of 0.5 MPa. The height of the gas collection chamber was 30 cm. The water depth was approximately 160 cm in the experiments.

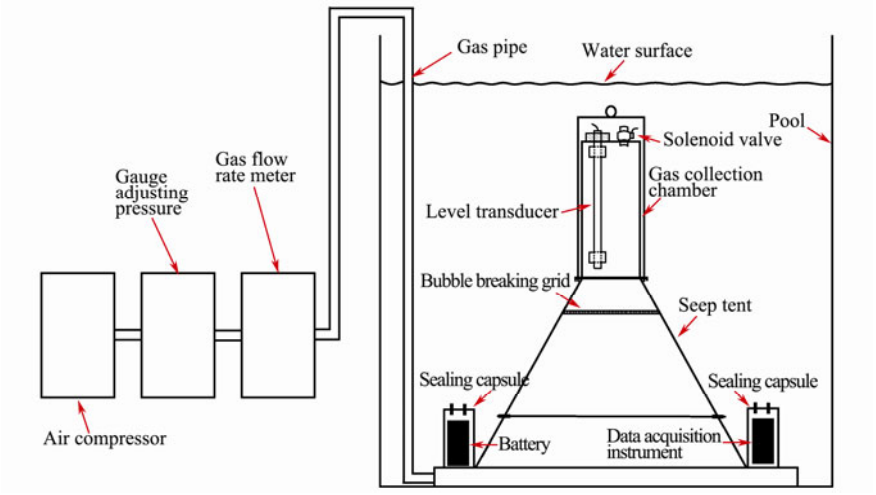

Fig.5 Schematic diagram showing the principles of the experimental facility.

According to the theory of the GFM device, the minimum measurable value of the gas flow rate of the GFM device should be close to 0 L min^{-1}, whereas the maximum value should be related to the time required for a single round of gas collection. As the shortest time was the time interval required for the opening and closing of the solenoid valve, which was no more than 3 s, the maximum measurable value of the gas flow rate should equal 34.5 L min^{-1}. However, we found that the gas flow rate of the GFM device never reached this value in the test experiment.

During the measurement experiment, two problems arose. The first was that upwelling gas bubbles could cause the probes of the level transducer to shake slightly, resulting in the opening and closing of the solenoid valve while the chamber collected gas; consequently, the GFM device did not work properly. To resolve this problem, we set an anti-shake time interval in the data storage and control system (akin to a camera with manual image stabilization). The optimal anti-shake time interval was 5 s. The second problem was that when a gas bubble erupted, the probes of the level transducer suddenly dropped down. This is because the gas bubble eruption may have caused the bubbles to coalesce, resulting in the solenoid valve opening continuously. Therefore, we considered the maximum gas flow rate of the GFM device as 15 L min^{-1}.

To quantify the relative error, the total gas flux and instantaneous flow rates were measured and recorded by the flow integrating instrument and the data storage and control system, respectively, for several hours at each flow rate setting. The measured instantaneous flow rates were averaged and the relative error was accurately cal-

culated by comparing the results obtained from the gas mass flow meter with those from the GFM device. The total flux (V_1) was calculated using Boyle's law, $P_1V_1/T_1 = P_2V_2/T_2$, where P_1 and P_2 are the atmospheric pressure and hydrostatic pressure, respectively, at the chamber depth; T_1 and T_2 are the same at room temperature; and V_2 is the gas volume measured by the chamber. We also investigated the effects of tent tilt angle and location of the bubble stream within the tent on the measurement results. We found that the wire bubble breakup grid had no significant effect on the upwelling flow. The effect of tilting the GFM device at small angles was also negligible.

Results from the calibration experiments are shown in Table 1. When the instantaneous gas flow rates of the gas mass flow meter were 50.3 mL min^{-1}, 100.6 mL min^{-1}, 150.9 mL min^{-1}, and 196.17 mL min^{-1}, the relative errors of the GFM device were approximately −3.4%, −0.28%, 0.55%, and −1.1%, respectively; the lower the instantaneous flow, the greater the relative error. This might be a result of the gas flow meter having a larger error at a lower flux. Therefore, we assumed that the relative error to be ± 1.0%.

Table 1 Relative error results of the GFM device from the calibration experiments

Flow rate	Time interval	Averaged flux*	Total flux	Total flux*	Relative error
50.3 mL min^{-1}	1566 s	48.66 mL min^{-1}	9.2 L	8.9 L	−3.3%
100.6 mL min^{-1}	761 s	100.13 mL min^{-1}	12.7 L	12.7 L	−0.3%
150.9 mL min^{-1}	501 s	152.096 mL min^{-1}	92.2 L	92.7 L	0.6%
196.17 mL min^{-1}	388 s	195.39 mL min^{-1}	12.8 L	12.7 L	−1.1%

Note: *denotes the total flux and average flux measured by the GFM device.

4 Field Deployment

4.1 Site Description

The Yinggehai Basin, located to the southwest of Hainan Island (at 16°50′–20°00′N and 107°–111°50′E), is one of the most gas-rich Cenozoic rift basins on the north shelf of the South China Sea. Here, there are five major seepage zones: Lingtou Promontory, Yinggehai Rivulet Mouth, Yazhou Bay, Nanshan Promontory, and Tianya Promontory. In this region, bubbles rise to the sea surface to form a near-shore bubble zone (Fig.1) (Huang *et al*., 2009). In the Lingtou Promontory seep field, more than 20 hydrocarbon seeps are found at a water depth from 3 to 5 m (Di *et al*., 2014a). Gas bubbles are clearly observed on the seafloor and sea surface, with a single gas bubble being up to 1–2 cm in diameter (Di *et al*., 2014a). The gas, primarily thermogenic methane, originates from the Miocene source rock in the central depression of the Yinggehai Basin (Huang *et al*., 2009).

4.2 Deployment and Recovery

On April 22, 2012, the fully assembled GFM device was deployed from a fishing vessel and placed over a hydrocarbon seep at Lingtou Promontory, approximately 300 m offshore, near Lingtou, Hainan province (Fig.1) (Di *et al*., 2014a, 2014b). It was recovered by divers on May 22, 2012. The GFM device was oriented in a fully upright position, and it showed minimal biofouling by organisms. Before removal of the GFM device, the solenoid valve had corroded and so it could not seal the collection chamber and the gas was not retained. During retrieval, the gas that was sealed in the collection chamber was boiling upward. On a subsequent dive during the same cruise, three replacement GFM devices were successfully deployed at different hydrocarbon seeps. It should be noted that because of unavoidable weather problems, although the GFM devices were deployed on the seafloor for 30 days, the measurement period was only 18 d.

5 Results and Discussion

5.1 GFM Design Assessment

The GFM device was assessed immediately after seafloor retrieval. Visually, the gas collection chamber and level transducer appeared to be in good condition, with no corrosion. However, the solenoid valve had corroded owing to extended deployment on the seafloor. Upon retrieval of the GFM device, it was found that the solenoid valve was not sufficiently well connected to seal the upwelling gas because of the magnetic soil. However, we assumed that the GFM device worked effectively before solenoid valve corrosion and that the results obtained for gas flow rate and total gas flux were accurate. We would like to note that a subsequent, improved GFM device contains an internal solenoid valve to minimize corrosion. We conclude that the GFM device is a promising tool for quantifying the long-term, *in situ*, and online methane flux from hydrocarbon seeps.

5.2 Gas Flux and Control Factor

Fig.6a shows the variation in gas flux and water depth measured continuously for about 18 d by the GFM device at the seep field (Di *et al*., 2014a, 2014b). The gas flux ranged from 0.36 to 1.25 L min^{-1} (22.36 to 72.24 L h^{-1}), which is much higher than the range of 0.28–0.43 L h^{-1} measured by Huang *et al*. (2009). The water depths at the hydrocarbon seep field ranged from 2.4 to 4.6 m (Fig.6). The gas flux trend was significantly negatively correlated with water depth, which was induced by ocean tides and swells. The correlation ($R^2 = 0.914$) between gas flux and water depth also reveals that gas flux is controlled by water depth (Di *et al*., 2014b). Each additional meter of sea height represents a hydrostatic pressure increase of 10^4 Pa and a natural gas flow rate decrease of 20–30 L h^{-1} (Di *et al*., 2014b). High tide was correlated with low flow rate, and vice versa (Fig.6). Similar results have been

observed at Hydrate Ridge, Bahía Concepción, and Baja California Sur as well as at 20 m water depth at Shane Seep in the Coal Oil Point seep field near Santa Barbara, California (Boles *et al*., 2001; Forrest *et al*., 2005; Torres *et al*., 2002). Therefore, our results clearly indicate that the seep gas flux in the fracture channel rapidly increases with the decreasing hydrostatic pressure induced by tides and swells. Furthermore, the period of bubble formation decreases and the number of bubbles formed increases, whereas the fracture pressure decreases until equilibrium is restored (Leifer *et al*., 2005; Di *et al*., 2014b). However, due to fracture resistance, fracture pressure may not decrease as fast as hydrostatic pressure; therefore, the gas flux may gradually increase. Conversely, an increase in hydrostatic pressure has the opposite effect (Leifer *et al*., 2005; Di *et al*., 2014b). Therefore, pore activation may be the dominant factor controlling the variations in gas flux (Boles *et al*., 2001; Leifer *et al*., 2005).

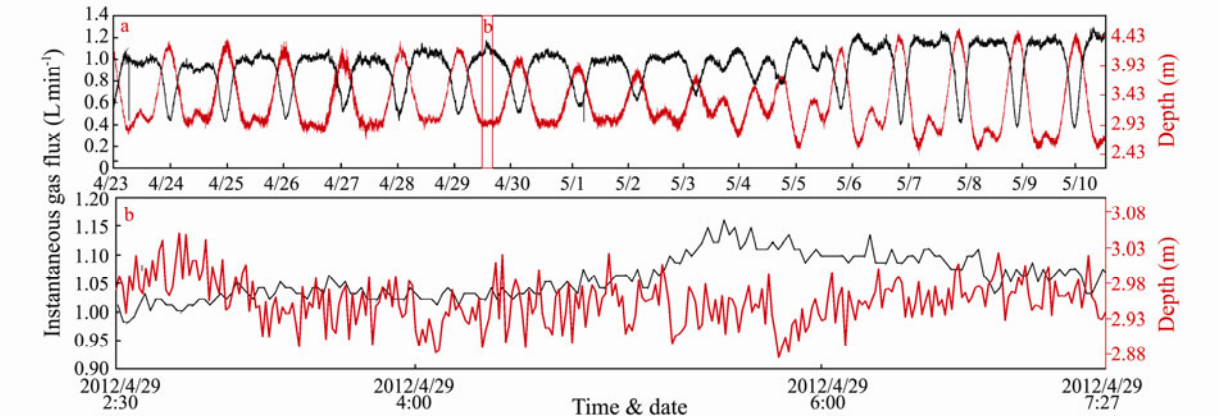

Fig.6 Time series of instantaneous gas flux (black line) and water depth (red line) at the Lingtou Promontory seep field (Di *et al*., 2014a).

The amount of gas measured by the GFM device was 30.5 m^3, resulting in a total gas flux of 6.36 × 10^2 $m^3 yr^{-1}$ from the seep vent (Di *et al*., 2014a). According to the bubble diameter (d = 1–2 cm) and methane content (95%) upon reaching the sea surface (McGinnis *et al*., 2006), it is speculated that a total of 4.84×10^4 to 6.84×10^4 $m^3 yr^{-1}$ (or 2.163×10^6 to 3.057×10^6 mol yr^{-1}) of methane is emitted from approximately 120 hydrocarbon seeps in this region (assuming that each hydrocarbon seep emits a similar gas flux) (Di *et al*., 2014a). This range is much higher than the preliminary calculated range (294–956 m^3 yr^{-1}) and the estimated values from other gas hydrate and upwelling study areas offshore SW Taiwan in the South China Sea (Chuang *et al*., 2006, 2010; Huang *et al*., 2009).

6 Conclusion

In this paper, we presented a detailed description of a new and inexpensive device to measure gas fluxes from hydrocarbon seeps. The device is an in situ and online gas measuring system that can be deployed at water depths of up to 3000 m. The device was used to quantify gas flux from hydrocarbon seep sites via the process of equal volume exchange. Limitations of the device might include gas hydrate formation in the chambers placed at methane seeps in the gas hydrate stability zone. Because power can be readily supplied, long-term in situ and online observations are possible. The inexpensive nature of the design facilitates the deployment of multiple units in the same area. After revamping, we will deploy more than three GFM devices at the Lingtou Promontory seep field for more than one year, and we will modify the structure of the GFM device such that it can be deployed at the active cold seep in the Northern South China Sea.

The device was successfully deployed on April 22, 2012 and recorded fluxes in the Lingtou Promontory seep field of the South China Sea for 18 d. The results revealed that the gas flux was controlled by the hydrostatic pressure induced by tides and swells. Based on the seep frequency response and the correlation between the gas flux and water depth, pore activation is considered to be the dominant controlling factor.

Acknowledgements

Financial support was provided by the National Scientific Foundation of China (Nos. 41676046 and 41306045), the Knowledge Innovation Project of the Chinese Academy of Sciences (Nos. SIDSSE-201208 and SQ201110), and the ‘Hundred Talents Program’ of the Chinese Academy of Sciences. The authors gratefully acknowledge financial support from China Scholarship Council.

References

Boetius, A., and Wenzhofer, F., 2013. Seafloor oxygen consumption fuelled by methane from cold seeps. *Nature Geoscience*, **6** (9): 725-734, DOI: 10.1038/ngeo1926.

Boles, J. R., Clark, J. F., Leifer, I., and Washburn, L., 2001. Temporal variation in natural methane seep rate due to tides. Coal Oil Point area, California. *Journal of Geophysics Research*, **106** (C11): 27077-27086, DOI: 10.1029/2000JC000774.

Brown, A., 2000. Evaluation of possible gas microseepage mechanisms. *American Association of Petroleum Bulletin*, **84** (11): 1775-1789, DOI: 10.1306/8626C389-173B-11D7-8645

000102C1865D.

Campbell, K. A., 2006. Hydrocarbon seep and hydrothermal vent paleoenvironments and paleontology: Past developments and future research directions. *Palaeogeography*, *Palaeoclimatology*, *Palaeoecology*, **232** (2-4): 362-407, DOI: 10.1016/ j.palaeo.2005.06.018.

Chen, D. F., Su, Z., and Cathles, L., M., 2006. Types of gas hydrates in marine environments and their thermodynamic characteristics. *Terrestrial Atmospheric and Oceanic Sciences*, **17** (4): 723-737.

Chen, D. X., Wu, S. G., Dong, D. D., Mi, L. J., Fu, S. Y., and Shi, H. S., 2013. Focused fluid flow in the Baiyun Sag, northern South China Sea: Implications for the source of gas in hydrate reservoirs. *Chinese Journal of Oceanology and Limnology*, **31**: 178-189, DOI: 10.1007/s0034 3-013-2075-5.

Chuang, P. C., Yang, T. F., Lin, S., Lee, H. F., Lan, T. F., Hong, W. L., Liu, C. S., Chen, J. C., and Wang, Y., 2006. Extremely high methane concentration in bottom water and cored sediments from offshore southwestern Taiwan. *Terrestrial Atmospheric and Oceanic Sciences*, **17** (4): 903-920.

Di, P. F., Feng, D., and Chen, D. F., 2014a. *In-situ* and on-line measurement of gas flux at a hydrocarbon seep from the northern South China Sea. *Continental Shelf Research*, **81**: 80-87, DOI: 10.1016/j.csr.2014.04.001.

Di, P. F., Feng, D., and Chen, D. F., 2014b. Temporal variation in the natural gas seep rate and the influence factors in the Lingtou promontory seep field of the northern South China Sea. *Terrestrial Atmospheric and Oceanic Sciences*, **25** (5): 665-672, DOI: 10.3319/TAO.2014.0 4.30.01(Oc).

Di, P. F., Huang, H. G., Huang, B. J., He, J. X., and Chen, D. F., 2012. Seabed pockmark formation assiociated with mud diapir decelopment and fluid activities in the Yinggehai Basin of the South China Sea. *Journal of Tropical Oceanography*, **31**: 26-36 (in Chinese with English abstract).

Dimitrov, L., 2003. Mud volcanoes − A significant source of atmospheric methane. *Geo-Marine Letter*, **23** (3-4): 155-161, DOI: 10.1007/s00367-003-0140-3.

Etiope, G., 2009. Natural emissions of methane from geological seepage in Europe. *Atmospheric Environment*, **43** (7): 1430-1443, DOI: 10.1016/j.atmosenv.2008.03.014.

Etiope, G., and Milkov, A., 2004. A new estimate of global methane flux from onshore and shallow submarine mud volcanoes to the atmosphere. *Environmental Geology*, **46** (8): 997-1002, DOI: 10.1007/s00254-004-1085-1.

Etiope, G., Christodoulou, D., Kordella, S., Marinaro, G., and Papatheodorou, G., 2013. Offshore and onshore seepage of thermogenic gas at Katakolo Bay (Western Greece). *Chemical Geology*, **339**: 115-126, DOI: 10.1016/j.chemgeo.2012. 08.011.

Etiope, G., Lassey, K. R., Klusman, R. W., and Boschi, E., 2008. Reappraisal of the fossil methane budget and related emission from geologic sources. *Geophysical Research Letters*, **35** (9): L09307, DOI: 10.1029/2008GL033623.

Feng, D., and Chen, D. F., 2015. Authigenic carbonates from an active cold seep of the northern South China Sea: New insights into fluid sources and past seepage activity. *Deep Sea Research Part II*: *Topical Studies in Oceanography*, **112**: 74-83, DOI: 10.1016/j.dsr2.2015.02.003.

Forrest, M. J., Ledesma-Vázquez, J., Ussler, Iii. W., Kulongoski, J. T., Hilton, D. R., and Greene, H. G., 2005. Gas geochemistry of a shallow submarine hydrothermal vent associated with the El Requesón fault zone, Bahía Concepción, Baja California Sur, México. *Chemical Geology*, **224** (1-3): 82-95, DOI: 10.1016/ j.chemgeo.2005.07.015.

Greinert, J., and Nutzel, B., 2004. Hydroacoustic experiments to establish a method for the determination of methane bubble fluxes at cold seeps. *Geo-Marine Letters*, **24**: 75-85, DOI: 10.1007/s00367-003-0165-7.

Han, X. Q., Suess, E., Huang, Y. Y., Wu, N. Y., Bohrmann, G., Su, X., Eisenhauer, A., Rehder, G., and Fang, Y., 2008. Jiulong methane reef: Microbial mediation of seep carbonates in the South China Sea. *Marine Geology*, **249** (3-4): 243-256, DOI: 10.1016/j.margeo.2007.11.012.

Hu, Y., Feng, D., Liang, Q. Y., Xia, Z., Chen, L. Y., and Chen, D. F., 2015. Impact of anaerobic oxidation of methane on geochemical cycle of redox-sensitive elements at cold seep sites of the northern South China Sea. *Deep Sea Research Part II: Topical Studies in Oceanography*, **122**: 84-94, DOI: 10.1016/ j.dsr2.2015.06.012.

Huang, B. J., Xiao, X. M., Hu, Z. L., and Yi, P., 2005. Geochemistry and episodic accumulation of natural gases from the Ledong gas field in the Yinggehai Basin, offshore South China Sea. *Organic Geochemistry*, **36** (12): 1689-1702, DOI: 10.1016/j.orggeochem.2005.08.011.

Huang, B. J., Xiao, X. M., Li, X. S., and Cai, D. S., 2009. Spatial distribution and geochemistry of the nearshore gas seepages and their implications to natural gas migration in the Yinggehai Basin, offshore South China Sea. *Marine and Petroleum Geology*, **26** (6): 928-935, DOI: 10.1016/j.marpetgeo. 2008.04.009.

Huang, B. J., Xiao, X. M., Li, X. X., 2003. Geochemistry and origins of natural gases in the Yinggehai and Qiongdongnan basins, offshore South China Sea. *Organic Geochemistry*, **34**(7): 1009-1025, DOI: 10.1016/S0146-6380(03)00036-6.

Huang, B. J., Xiao, X. M., Zhu, W. L., 2004. Geochemistry, origin, and accumulation of CO_2 in natural gases of the Yinggehai Basin, offshore South China Sea. *American Association of Petroleum Geologists Bulletin*, **88** (9): 1277-1293, DOI: 10.1306/04120403045.

Huang, C. Y., Chien, C. W., Zhao, M. X., Li, H. C., and Lizuka, Y., 2006. Geological study of active cold seeps in the syncollision accretionary prism Kaoping Slope off SW Taiwan. *Terrestrial*, *Atomospheric and Oceanic Sciences*, **17** (4): 679-702.

Judd, A. G., 2003. The global importance and context of methane escape from the seabed. *Geo-Marine Letter*, **23** (3-4): 147-154, DOI: 10.1007/s00367-003-0136-z.

Judd, A. G., 2004. Natural seabed gas seeps as sources of atmospheric methane. *Environmental Geology*, **46** (8): 988-996, DOI: 10.1007/s00254-004-1083-3.

Judd, A. G., and Hovland, M., 2007. *Submarine Fluid Flow*, *the Impact on Geology*, *Biology*, *and the Marine Environment*. Cambridge University Press, Cambridge, UK, 475pp.

Judd, A. G., Hovland, M., Dimitrov, L. I., García, Gil. S., and Jukes, V., 2002. The geological methane budget at Continental Margins and its influence on climate change. *Geofluids*, **2** (2): 109-126, DOI: 10.1046/j.1468-8123.2002.00027.x.

Leifer, I., 2015. Seabed bubble flux estimation by calibrated video survey for a large blowout seep in the North Sea. *Marine and Petroleum Geology*, **68**: 743-752, DOI: 10.1016/j.marpe tgeo.2015.08.032.

Leifer, I., and Boles, J., 2005. Turbine tent measurements of marine hydrocarbon seeps on subhourly timescales. *Journal of Geophysics Research*, **11**0 (C1): C01006, DOI: 10.1029/ 2003JC002207.

Leifer, I., and MacDonald, I., 2003. Dynamics of the gas flux from shallow gas hydrate deposits: Interaction between oily hydrate bubbles and the oceanic environment. *Earth and*

Planetary Science Letters, **210** (3-4): 411-424, DOI: 10.1016/S0012-821X(03)00173-0.

Li, C. P., Liu, X., Yang, L., He, J., and Lu, L., 2010. Study on the bubble radius and content effect on the acoustic velocity of seawater with bubbles. *Geoscience*, **24** (3): 528-533 (in Chinese with English abstract).

Li, L., Lei, X. H., Zhang, X., and Sha, Z. B., 2013. Gas hydrate and associated free gas in the Dongsha Area of northern South China Sea. *Marine and Petroleum Geology*, **39**: 92-101, DOI: 10.1016/j.marpetgeo.2012.09.007.

Liang, Q., Hu, Y., Feng, D., Chen, L., Yang, S., Liang, J., Tao, J., and Chen, D., 2016. Authigenic carbon-ates from two newly discovered active cold seeps on the northwest-ern slope of the South China Sea: Constraints on fluids sources, formation environments and seepage dynamics. *Deep Sea Research* I, Under Revision.

Long, J. J., Huang, W., Zou, D. P., Di, P. F., Wu, J. P., 2012. Method of measuring bubble flow from cool seeps on seafloor using acoustic transmission and preliminary experiments. *Journal of Tropical Oceanography*, **31**: 100-105 (in Chinese with English abstract).

McGinnis, D. F., Greinert, J., Artemov, Y., Beaubien, S. E., and Wüest, A., 2006. Fate of rising methane bubbles in stratified waters: How much methane reaches the atmosphere? *Journal of Geophysics Research*, **111** (C9): C09007, DOI: 10.1029/2005JC003183.

Nikolovska, A., and Waldmann, C., 2006. Passive acoustic quantification of underwater gas seepage. *OCEANS* 2006, 1-6, DOI: 10.1109/OCEANS.2006.306926.

Roberts, H., Wiseman, W. J., Hooper, J., and Humphrey, G., 1999. Surficial gas hydrates of the Louisiana continental slope-initial results of direct observations and *in situ* data collection. *Proceedings of the Annual Offshore Technology Conference*, Houston, Texas, 10770pp.

Roberts, H. H., 2001. Fluid and gas expulsion on the northern gulf of mexico continental slope: Mud-prone to mineral-prone responses. In: *Natural Gas Hydrates*: *Occurrence*, *Distribution, and Detection*. Charles, K. P., ed., 1st edition, *American Geophysical Union*, USA, 145-161.

Suess, E., 2014. Marine cold seeps and their manifestations: Geological control, biogeochemical criteria and environmental conditions. *International Journal of Earth Science*, **103** (7): 1-28, DOI: 10.1007/s00531-014-1010-0.

Torres, M. E., McManus, J., Hammond, D. E., de Angelis, M. A., Heeschen, K. U., Colbert, S. L., Tryon, M. D., Brown, K. M., and Suess, E., 2002. Fluid and chemical fluxes in and out of sediments hosting methane hydrate deposits on Hydrate Ridge, OR, I: Hydrological provinces. *Earth and Planetary Science Letters*, **201** (3-4): 525-540, DOI: 10.1016/S0012-821X(02)0073 3-1.

Von Deimling, J. S., Greinert, J., Chapman, N. R., Rabbel, W., and Linke, P., 2010. Acoustic imaging of natural gas seepage in the North Sea: Sensing bubbles controlled by variable currents. *Limnology and Oceanography Methods*, **8**: 155-171, DOI: 10.4319/lom.2010.8.155.

Wang, B., and Socolofsky, S. A., 2015. A deep-sea, high-speed, stereoscopic imaging system for in situ measurement of natural seep bubble and droplet characteristics. *Deep Sea Research Part I: Oceanographic Research Papers*, **104**: 134-148, DOI: 10.1016/j.dsr.2015.08.001.

Wang, B., Socolofsky, S. A., Breier, J. A., and Seewald, J. S., 2016. Observations of bubbles in natural seep flares at MC 118 and GC 600 using in situ quantitative imaging. *Journal of Geophysical Research*: *Oceans*, **121**: 2203-2230, DOI: 10.1002/2015JC011452.

Washburn, L., Johnson, C., Gotschalk, C. C., and Egland, E. T., 2001. A gas-capture buoy for measuring bubbling gas flux in oceans and lakes. *Journal of Atmospheric and Oceanic Technology*, **18**: 1411-1420, DOI: 10.1175/1520-0426(2001)018<1411:AGCBFM>2.0.CO;2.

(Edited by Ji Dechun)